ISSN 0915-633X

NATIONAL INSTITUTE FOR FUSION SCIENCE

Optimization of Cs Deposition in the 1/3 Scale Hydrogen Negative Ion Source for LHD-NBI System

Y. Oka, Y. Takeiri, Yu.I.Belchenko, M. Hamabe, O. Kaneko,
K. Tsumori, M. Osakabe, E. Asano,
T. Kawamoto and R. Akiyama

(Received - Oct. 15, 1999)

NIFS-620 Dec. 1999

RESEARCH REPORT
NIFS Series

NAGOYA, JAPAN

Optimization of Cs deposition in the 1/3 scale Hydrogen Negative Ion Source for LHD-NBI system

Y.Oka[1)], Y.Takeiri[1)], Yu.I.Belchenko[2)], M.Hamabe[3)], O.Kaneko[1)], K.Tsumori[1)], M.Osakabe[1)], E.Asano[1)], T.Kawamoto[1)], R.Akiyama[1)]

[1)]National Institute for Fusion Science, Toki-city, 509-5292, Japan
[2)] Budker Institute of Nuclear Physics, Novosibirsk, 630090, Russia
[3)] Chubu University, Kasugai-city 487-8501, Japan

Abstract

A compact cesium deposition system was used for direct deposition of cesium atoms and ions onto the inner surface of the 1/3 scale Hydrogen Negative Ion Source for the LHD-NBI system. A small, well defined amount of cesium deposition in the range of 3-200 mg was tested. Negative ion extraction and acceleration were carried out both in the pure hydrogen operation mode and in the cesium mode. Single Cs deposition of 3-30 mg to the plasma chamber have produced temporary 2-5 times increases of H- yield, but the yield was decreased within several discharge pulses to the previous steady-state value. Two consecutive 30 mg depositions done within a 3-5 hours/ 60 shot interval, produced a similar temporary increase of H- beam, but reached a larger H- yield steady-state value. Deposition of larger 0.1-0.2 g Cs portions with a 20-120 hours/ 150-270 shot interval improved the H- yield for a long (2-5 days) period of operation. Directed depositions of Cs to the various walls of the plasma chamber showed approximately the same H- increase. Deposition of 0.13 g Cs to a surface polluted by a water leak, produced a temporary increase, and an H- steady-state level similar to that from a single 30 mg cesium deposition. Deposition of 0.1 g with a cesium plasma produced one half the H- yield obtained by deposition of the same amount of cesium atoms. A higher steady-state H- current value and a smaller rate of H- yield decrease was recorded during the 8 filaments discharge operation, as compared to the 12 filaments operation at the same discharge power.

Keywords: hydrogen negative ion, ion source, cesium deposition, NBI

Cesium seeding of the hydrogen discharge of a Multicusp Sources (MS) of Negative Ions (NI) remarkably improves the source parameters and permits development of MS based neutral injectors for fusion devices[1-3]. Experimental evidence indicates[4-8] that cesium deposition to the Plasma Grid (PG) is responsible for H- yield improvement. The study of NI production with direct deposition of cesium onto MS internal walls was done recently at the National Institute for Fusion Study. These experimental data and the experiments on cesium recovery from polluted layers in the internal walls[9] confirm the surface origin of NI yield improvement in the MS[10] and show that a dynamic cesium-tungsten coverage of the PG surface supports the enhanced H- production. The results of a NI production study with direct deposition of well-defined cesium amounts are described below.

A. Experimental Setup

In the cesium deposition experiments, an external-filter-type 1/3 scale large NI source was used, which has been developed for high-energy and high-current beam production. The detailed source and test stand structure are described in Ref.3. Fig.1 shows a schematic diagram of the 1/3 scale ion source with a one stage accelerator and with the cesium oven introduced into the source volume. The plasma source dimensions are 35^{W}x 69^{H} x 20^{L} cm^3. Directly heated tungsten filaments (12,10 or 8) are used for electron emission to form a discharge. There are three grids used for H- beam extraction and acceleration - plasma grid (PG), extraction grid, and grounded grid. The PG has 270 apertures of 9 mm in diameter, with a total grid area of 25x26 cm. The ion source is attached to the negative-ion-based NBI test stand. The test stand has two large vacuum chambers: the ion source chamber and the beam dump chamber, connected to each other via a 5-m-long neutralizer. Two multichannel calorimeter arrays, located 5 m (#1) and 11.2 m (#2) downstream from the ion source, are employed for total H- ion current measurement, using the horizontal and vertical profiles obtained in one shot. H^- beam acceleration up to 90 keV with beam pulse duration 0.6-1.3 s was used. The optimal ratio of the extracted and accelerated voltages was 1:12. About 2.5 A H- current produced with the 1/6 scale extraction area of 25x26 cm^2 from the 1/3 scale source at 50 kW arc power corresponds to 40 A H- yield for the full-scale source[3].

The cesium deposition system consisted of a small detachable oven[11] mounted on a feedthrough with a double-valve vacuum lock device. It permited the oven to be placed into or removed from the vacuum box without introducing air into the source, as well as rotation and movement of the oven along the length of the discharge chamber. Special pellets containing a mixture of cesium chromate (30 %) and titanium (70 %) were used for cesium release. The pellets have a low sensitivity to contamination by air, and can be reloaded under atmospheric pressure. A cesium stream, ejected from the oven outlet with a total divergence of about 90° is produced at the oven temperature 1000-1100 K. No accompanying "poisoning" impurities release (oxygen, water) was observed during oven heating for cesium release.

The oven was placed into the source through a small port in the anode bottom with the help of a long feedthrough stick. The cesium deposition was usually produced with the oven's cesium outlet oriented towards the Plasma Chamber (PC) back or side walls to prevent direct injection of the cesium into extraction-acceleration channels. The cesium transport to the PG surface occurred due to cesium thermal desorption and sputtering by discharge particles. Localized cesium deposition to the small area (about 10 cm in diameter) of the back wall was obtained with the oven outlet oriented towards the PC back. About 0,1 m^2 area of the back wall was deposited with cesium when the oven was turned at an angle of $\pm 30^0$ with respect to back wall. Oven turning and a 50 cm shift along the vertical axis permited cesium deposition to most parts of the PC side and back surfaces.

The Cs deposition was usually done under vacuum conditions during a 30-50 minute injection pause between the discharge pulses. Conditioning of source surfaces by hydrogen discharges was usually done before cesium deposition. The amount of deposited cesium was varied according to the number of pellets loaded, oven temperature, and heating interval change. Total cesium yield from the oven was limited by the amount of pellets loaded to the oven: this was varied in the range 3 mg - 0.2 g. A pellet with 2,4 mm diameter and 0.8 mm thickness provides about 0.7 mg of cesium release. An atmosphere of gaseous argon was introduced into the source volume during a pause in the operation or before PC evacuation to air.

Cesium deposition with a cesium plasma gun was also tested. A special cesium ionizing unit was capped to the oven for production of the cesium plasma. The cesium atom flux from the oven entered the unit volume and was ionized by a dc arc ignited with the help of an internal electrode having an anode potential. The directed flux of cesium plasma (with a total divergence of about 60°) was injected from a side wall gun nozzle having a cathode potential. No biasing of the unit body with respect to PC walls was applied in these first experiments. Total cesium flux from the gun was controlled by the oven temperature. The cesium ionization rate was controlled by the discharge power supply. The arc current/ voltage of the unit was varied from 10-50 mA/30-40 V at cesium fluxes 0.01-0.1 mg/min up to values 1-1.3 A/ 7-8 V with cesium flux growth to 1-3 mg/min. 100 mg Cs deposition was produced during about 1 hour of arc unit operation with a gradual increase of oven temperature to allow for complete cesium release. Most of the cesium was deposited in a low voltage arc mode, with a low energy flux of cesium ions.

B. EXPERIMENTAL RESULTS

H- production with 3-30 mg Cesium Depositions

1. The H- beam production with a 3 mg cesium deposition to PG top and bottom parts having no emission apertures was tested first. Only 5 cesium pellets were loaded into the oven in this case. The oven nozzle was positioned 21 cm above the central axis of the source and it was oriented towards the PG. About half of the cesium amount was deposited to the PG upper side with the oven turning around its axis for cesium spreading within an angle ±45° with respect to the PG normal. Then the oven was positioned 21 cm below the central axis, and the rest of the cesium was deposited to the PG. Then the oven was removed from the MS volume, and the source was switched on into the H- beam production regime. Fig.2 shows the evolution of accelerated H- beam current, measured by calorimeter 1, as a function of shot number after the cesium deposition for three cases of small cesium deposition. Data for the first 3 mg deposition are shown in Fig.2 by circles. The H- extraction/ acceleration voltage was applied starting the 9th shot after cesium deposition. In the 9th -12th shots the H- yield had a value similar to that of the pure hydrogen mode (discharge power in the 9th -12th shots had a lower value of 30-39 kW). The effect of cesium on H- production started to appear at the 13th shot after cesium deposition, when the H- yield increased to the value of about 0.8 A at a PG temperature of 180 °C, measured by the thermocouple on the PG periphery. Then H- current decreased quickly to the previous (pure hydrogen) level of about 0.6 A (at a hydrogen filling pressure of about 0.4 Pa and at a discharge power of 50 kW) with further operation.

The other 3 mg cesium deposition was done to the west and east long side walls of the PC after 270 shots, on the next day, with the oven nozzle at positions 10 cm higher and 10 cm below the central axis. The extraction/acceleration voltage was applied starting the 11th shot after this deposition. H- beam current had a maximal value in this 11th shot, and it again decreased quickly with the shot number increase (this deposition is not shown in Fig.2).

After producing 170 shots the next 3 mg cesium deposition to the west and east side parts of the PC was done. The data on H- production in this case are shown in Fig.2 by crosses, and the corresponding values of PG temperature, are shown by triangles. The initial level of H- current at a discharge power of 50 kW was about 0.7 A due to higher discharge hydrogen filling pressure of 0.7 Pa. The beam extraction/acceleration voltage was switched on, starting the first discharge shot after the cesium deposition. As is shown in Fig.2, the effect of cesium on H- production enhancement appeared in the first shots after the cesium deposition. H- beam current had a maximal value of about 1.25 A in the 3rd shot after cesium deposition, at PG temperature of about 150 °C, and it decreased gradually to the H- «pure hydrogen» level 0.7 A during a few tens of shots.

2. The similar temporary increase of H- beam current is displayed after the next three 10-30 mg cesium depositions, done with the intervals 3-16 hours between the consecutive depositions (Fig.3, 50 kW, 0.7 Pa shots). The case of 10 mg deposition to PC west/east sides, made with the interval 4 hours / 100 shots after the described 3 mg deposition, is shown in Fig.3 by crosses. The residual value of H- beam current before deposition was about 0.7 A, H- yield had a maximal value of about 2.1 A in the 5-6th shots at PG optimal temperature of about 150 °C. Circles in Fig.3 illustrate the case of the 30 mg deposition to the same PC side, made with the interval 3 hours/40 shots after the former 10 mg case. The residual value of H- beam current before deposition was about 0.8 A, and H- yield had a maximal value of about 2-2.1 A in the 4-8th shots at the same PG optimal temperature 150 °C. The second 30 mg portion was deposited to the PC back side with 16 hours/ 110 shots interval, and the third 30 mg portion was deposited to plasma chamber back side with 3 hours/ 60 shots interval after the second one. Triangles in Fig.3 show the data after the third 30 mg cesium deposition (the second one not shown in Fig.3).The maximal H- beam current of about 2.1 A was achieved in the 7th-10th shots after deposition, at a PG optimal temperature of 170 °C, and the residual value of H- current (after the 57 pulses, before the next 0.1g deposition) was about 1 A. Cesium depositions to the PG top/down area, to the PC west/east sides and to the PC back side show approximately the same H- temporary increase and the same H- current steady-state value.

3. Two electrostatic probes which were situated at the various distance from the cesium deposition places were used for the control of discharge parameters in the source driver region before and after cesium directed depositions. Small increases of the plasma potential from 5 to 6 V with respect to anode was recorded by both probes after a 3 -30 mg cesium deposition. No change of electron temperature and plasma density was recorded in the source driver region in these cases. There was no difference in data for both probes.

0.1-0.15 g cesium depositions

1. Deposition of larger 0.1-0.2 g Cs portions with 20-120 hours/ 150-270 shots intervals between the depositions have demonstrated more stable enhancement of H- yield for a longer (2-5 days) period of operation (Fig.4). The first 0.1 g cesium deposition to the PC back (before the shot #1 in Fig.4), resulted in a temporary increase of H- beam current to 2 A value at the PG optimal temperature 200 °C, and were decreased to a residual value about 1.5 A in 10 shots with the PG further heating. This residual value was degraded to 1.2 A during 150 shots operation. The second deposition of 0.1 g cesium portion to PC back (produced before shot #170, with about 0.3 g total amount of deposited cesium in the 3 last days), resulted in a H- beam current increase to the

value of about 2.2 A at PG optimal temperature 200 °C, and to H- current temporal drop with PG temperature increase to 220 °C. After that, H- beam current recovered to a steady-state value of about 2.2 A. The H- steady-state value gradually decreased to 2 A after about 100 shots/2 days operation, and to 1.6 A - after 200 shots/3 days operation. Additional 0.2 g cesium deposition to the PC back (produced before shot #430 in Fig.4, with cesium total amount 0.5 g) resulted in H- beam current jump to 2.5 A at PG optimal temperature 200 °C, and then to H- current temporal drop down to 2.2 A with PG temperature increase to 220 °C. After the temporal drop, H- beam current recovered to a steady-state value of 2.6 A and gradually decreased to 2.3 A level in 2 days/140 shots of operation.

A similar jump of H- current up to 3.1 A was recorded after the next 0.1 g cesium deposition to the PC back (total deposited cesium amount 0.6 g during 6 days/900 shots operation). No steady-state H- current value was attained in this run because of an occasional water leak to the vacuum chamber. H- beam current decreased to a «pure hydrogen» value of 0.7 A after the pollution of deposited cesium by the water leak.

2. The values of the H- beam current temporary maximum at the 50th and the 100th shot after cesium depositions versus total deposited cesium amount are shown in Fig.5. The initial H- maximum sharply increased with total deposited cesium amount in the range 3-20 mg, and did not further change with cesium amount adding up to 0.3 g. The residual H- current value after 50 and 100 shots increased with the total deposited cesium amount first, and then saturated at a cesium deposit of about 0.6 g.

Operation with a decreased number of filaments

The previously described 3mg - 0.2 g cesium deposition was done with the 12 filaments discharge operation. Operation with 8 filaments (2 top and 2 down filaments were disconnected from the power supply) produces the similar temporary increase of H- yield in the case of small (10 mg) cesium deposition, but a larger and longer residual steady-state H- current for 0.1 - 0.15 g depositions. Namely, 0.1 g deposition (added to the previously deposited 10 mg) provides an increase of H- beam current to 2.8 A value, and then it gradually decreased to a 2 A level in 500 shots/2 days of operation. The next 0.15 g deposition produced a 2.8 A steady-state level of H- current for 300 shots/2 days operation.

H- current dependence on PG temperature

The increase of H- current to a maximal value at the optimal PG temperature occured every time after the cesium deposition or after a long (several hours) stop in operation with PG cooling down. No change of H- current with the change of PG temperature was recorded during operation while keeping the PG hot, as is shown in Fig.6. The evolution of H- current was recorded during the operation at the steady-state 1.2 A beam current value on the next day after 0.1 g cesium deposition (shots 90-150 of Fig.4). The interval between the shots was increased to 5 minutes, starting shot #90. It produces a decrease of PG temperature, but no change of H- current (Fig.6). The interval between the shots was decreased to 2 min, starting shot #120, and PG temperature increased back to the 250 °C level with no change of H- current. Similar insensitivity of H- current to PG temperature was recorded with the PG temperature increase during the enlargement of discharge pulse duration[12].

Cs deposition to the source, polluted by the water leak

The contamination of deposited 0.61 g of cesium by an occasional water leak resulted in a decrease of H- beam current down to about a pure hydrogen level after the test stand vacuum system recovery. Cesium deposition to the PC polluted surface was tested. Deposition of 0.13 g of cesium to the PC back polluted surface resulted in a temporary H- yield increase to 2.8 A, as measured by the second, distant calorimeter #2. The residual H- current value after 50 shots of operation was about 50% higher than that in the water-polluted source before the cesium deposition. The H- current evolution during the operation was similar to that, shown in Fig.3, for the third 30 mg cesium deposition run.

Cs deposition with the cesium plasma gun

The effect of cesium plasma deposition to the PC back on H- beam current is shown in Fig.7. Circles show the 0.1 g deposition onto the wiped, clean copper PC surfaces, initially conditioned by the pure hydrogen discharge. The evolution of H- beam current in this case was similar to those of the 10-30 mg cesium atom depositions. A temporary maximum of H- beam current had a value of 1.5 A at PG temperature 200 °C and it gradually decreased to 1 A value at the end of the day, and down to 0.8 A - on the next day. H- yield was about two times less as compared with the deposition of the same amount of cesium atoms. Triangles in Fig.7 show the case of the 0.1 g deposition with cesium plasma to the PC back into the previously cesiated (0.4 g) and well conditioned source. The residual H- beam current had a 2.3 A value before this additional deposition by cesium plasma. H- beam current decreased after this deposition with plasma. It had a temporary maximum of about 1.2 A after the deposition and conditioning by 50 discharge pulses, and then decreased to 0.7 A at the 80-th shot of operation. Further conditioning by discharges increased the H- beam current to the level of about 1.2 A, two times lower than the H- level before the deposition by plasma (Fig.7). The steady-state H- beam current has approximately the same value in both cases of cesium plasma deposition onto the wiped surface of PC back or

over the previously deposited to PC back Cs+W reservoir, having 0.4 g of cesium.

C. DISCUSSION

The described data on H- production with the directed deposition of cesium into the MS and the data on cesium recovery from the polluted layers in the MS[9] shows, that a dynamic cesium-tungsten coverage of PG surface supports the enhanced H- production[10].

The surface NI production is maximal at the optimal cesium coverage and it needs only a small amount of cesium on molybdenum (or tungsten) of about $\theta \sim 0.7 \approx 2\text{-}3 \cdot 10^{14}$ cm^{-2} ≈ 0.5-0.8 mg/m^2. The binding energy of cesium in this case is high (about 2-2.5 eV), so a low cesium volume pressure 10^{-6}-10^{-5} Pa is enough for supporting an optimal cesium coverage on the PG surface with temperature 200-250 °C.

Deposition of 3-30 mg of cesium into the 1/3 scale source produced a thick 5-50 layer average cesium coverage on the PC and PG surfaces with a total area of 0.8 m^2. At a water-cooled walls temperature of 18 °C a thick pure cesium layer supported a volume cesium pressure of about 10^{-4} Pa, and most of the cesium escaped in tens of minutes from the thick layer to the extractor through the emission apertures (pumping speed of cesium through the openings at this pressure is about 0.5 mg/min). Nevertheless only a trace of cesium was detected in the accelerator chamber after the long-term operation with multiple cesium depositions, while the main part of the injected cesium was collected in the thick cesium-tungsten layer on the PC and PG walls. It shows, that the deposited cesium is blocked on the PC walls by impurities (evaporated tungsten, residual water). This blocking increases the cesium binding to the surface and decreases the cesium escape from PC.

Deposition of 3-30 mg of cesium into a 1/3 scale source produces a temporary improvement of H- beam current for 10-20 shots/ 20-40 min of operation. This temporary increase of H- yield is caused by the optimization of cesium coverage on PG surface. After cesium deposition the cold PG surface is covered by a thick cesium layer, blocked by impurities. Initial increase of PG temperature provides the desorption of the cesium excess and of the contaminants from the PG surface. An optimal PG temperature corresponds to the maximal H- yield over the most parts of PG area. No change of the H- temporary maximum value with the increase of deposited cesium in the range 10 mg - 0.1 g (Fig.3,5) shows that these amounts of cesium are enough for producing an optimal cesium coverage over most of the PG area. A decreased value of H- current temporary maximum after several 3 mg cesium depositions can be caused by a non-uniform PG cesium coverage in these cases. Larger cesium amounts provide a higher cesium volume pressure and a partial compensation of the cesium losses during PG heating. As a result the larger cesium portions supply a longer operation with an increased H- current at a larger value of optimal PG temperature.

H- current decreased rapidly after the initial maximum during the further operation and the PG temperature growth because of the PG cesium coverage depletion and its blocking by tungsten, evaporated from filaments. As a result of the tungsten deposition, coverage on the PG becomes enriched by tungsten, and it decreases the H- production. The amount of this drop was insensitive to deposited cesium in the range 3 mg- 0.1 g. It shows that cesium PG coverage depletion at PG high temperatures dominates over cesium incoming flux.

The cesium escape from the optimal cesium coverage $\theta \sim 0.7$ on tungsten at temperature 200 °C has a rate of about $3 \cdot 10^{11}$ atoms/cm^{2}s, so about 10 min 200 °C temperature operation is needed for desorption of the bulk of the PG optimal cesium coverage. The rate of tungsten evaporation from filaments for the emission-limited discharge mode is about 0.2 mg for 1 kA, 5 sec filament heating pulse. It produces an average flux of about $4 \cdot 10^{13}$ atoms/cm^2 to the PC surface in one pulse, and a monolayer of tungsten will cover the PC surface after 20 shots. The indicated rate of the cesium overlaying by tungsten correlates with the measured rate of H- current drop after small cesium deposition.

Low residual value of H- current after 3-30 mg depositions and a 50 shots/2 hours operation shows, that cesium flux from the PC volume does not compensate the PG cesium coverage depletion/blocking. Small Cs deposits on anode surfaces are overlayed by the evaporated tungsten well, and it prevents the low work function PG coverage.

The increase of the residual value of H- current (after 50-100 shots/2-3 hour operation) proportionally to the total amount of the deposited cesium shows that the cesium replenishing flux to the PG hot surface (i.e. volume pressure) is proportional to the total deposited cesium. It confirms that most of the cesium is deposited on the PC walls, and that the rate of cesium blocking on PC walls is decreased with the cesium amount increase. The 0.1-0.2 g portion of Cs deposited to the 1/3 scaled source seemed enough for building the Cs reservoir, resistive to the total blocking by evaporated tungsten. Higher tungsten evaporation over a larger PC area during the 12 filaments non-uniform discharge operation produced a higher cesium blocking, than that during 8 filaments operation with the same discharge power. As a result, stable replenishment of PG surface by cesium from the reservoir supports the optimal Cs-W coverage on PG and a high steady-state level of H- beam production during hundreds of shots of 8 filaments operation.

The change of hot PG temperature during operation with a longer pause or with a shorter pulse length does not influence the H- yield. Longer pulse length (or shorter pause between pulses) increases the PG temperature and the cesium flux from PG coverage, but the equilibrium PG coverage does not change in this case because of an increased tungsten evaporation from the Cs+W coverage on the hot PG surface.

Cesium ions attached well to the surface during deposition with plasma. As a result, the smooth deposition of cesium ions onto the Cs-W reservoir at the PC back decreased the cesium volume pressure and the cesium replenishment on the PG surface. It decreased the H- production in the source, previously cesiated by atoms. Cesium plasma deposition to the wiped PC back provided a lower H- temporary increase and a lower H- steady-state level as compared with the deposition by cesium atoms to the PC back due to a decreased cesium replenishing from the Cs-W reservoir.

Cesium deposition to the surface, polluted by a water leak, produced the same temporary H- current increase, as in the case of deposition of the wiped surface, but a lower residual steady-state H- current level. It shows that both depositions supply similar optimal PG coverage on initial heating, but the replenishing cesium flux is lower from the cesium reservoir on the polluted surface.

SUMMARY

A dynamic cesium-tungsten coverage of the plasma grid surface supports an enhanced H- production in large Multicusp Sources. The tungsten blocking of the Cs layer decreases the cesium volume pressure and prevents the cesium escape from the source. A 100-200 mg Cs deposition is enough for stable improvement of source parameters for hundreds of shots of operation.

Literature

1. R.S.Hemsworth, J.-H.Feist, T.Inoue, E.Kussel, D.Murdoch, A.Panasenkov, K.Shibata, M.Tanii, and M.Watson. Proceedings of the 16th Symposium on Fusion Engineering, Vol.1 (1995), p.264
2. N.Miyamoto, H.Oguri, Y.Okumura, T.Inoue, Y.Fujiwara, K.Miyamoto, A.Nagase, Y.Ohara, and K.Watanabe. AIP Conf. Proc. No.380, New York, 1996, pp.300-306
3. O.Kaneko, Y.Oka, M.Osakabe, Y.Takeiri, K.Tsumori, R,Akiyama, E.Asano, T.Kuroda and A.Ando. Proceedings of the 16th Symposium on Fusion Engineering, Vol.2 (1995), p.1082
4. K.N.Leung, C.F.A. van Os, and W.B.Kunkel. Appl.Phys.Lett., **58**, 1467 (1991).
5. Y.Okumura, M.Hanada, T.Inoue, H.Kojima, Y.Matsuda, Y.Ohara, M.Seki, and K.Watanabe. AIP Conf. Proc., No 210 (AIP, New York, 1990), pp.169-180
6.Y.Mori, T.Okiyama, A.Takagi and D.Yuan. Nucl.Instrum.Meth., **A301**, 1 (1991).
7. C.Jacquot, D.Riz, R.Trainham, K.Miyamoto, Y.Okumura, M.Hopkins. Fusion Technology 1996, Elsevier Science (1997), p.677
8. C.Jacquot, J.Pamela, Yu.Belchenko and D.Riz. Rev.Sci.Instrum., **67**, 1036 (1996).
9. Yu.I.Belchenko, Y.Oka, O.Kaneko , Y.Takeiri, A.Krivenko, E.Asano K.Tsumori, T.Kawamoto, R.Akiyama. Rev.Sci.Instrum., these proceedings.
10. Yu.I.Belchenko, Y.Oka, O.Kaneko, Y.Takeiri, K.Tsumori. «On Mechanism of Negative Ion Production in the Large Hydrogen Negative Ion Sources» - to be published
11. Yu.Belchenko, C.Jacquot, J.Pamela and D.Riz. Rev.Sci.Instrum., **67**, 1033 (1996).
12. Y.Takeiri, M.Osakabe, Y.Oka, K.Tsumori, O.Kaneko, T.Takanashi, E.Asano, T.Kawamoto, R.Akiyama, and T.Kuroda. Rev.Sci.Instrum., **68**, 2012 (1997).

Figure Captions

Fig.1. A schematic diagram of the 1/3 scale ion source with the cesium oven introduced

Fig.2. H- beam current evolution after 3 mg cesium depositions
circles - first 3 mg deposition,
crosses - third deposition of 3 mg portion,
T - PG temperature in third 3 mg deposition (triangles).

Fig.3. H- beam current evolution after 10-30 mg cesium depositions.
1- 10 mg deposition (crosses),
2 - 30 mg portion (circles),
3 - third deposition of 30 mg portion (triangles).

Fig.4. H- beam current evolution after 0.1-0.2 g cesium depositions.
crosses, and triangles - 0.1 g depositions,
circles - 0.2 g deposition.

Fig.5. H- beam versus total deposited cesium amount
1 - at temporary maximum (crosses),
2 - at 50th shot after cesium depositions (circles)
3 - at 100th shot after cesium depositions (triangles)

Fig.6. H- current and PG temperature evolution during operation with a longer/shorter pause between the pulses.

Fig.7. H- beam current evolution after cesium deposition by plasma
circles - deposition to wiped wall
triangles - additional deposition over cesium

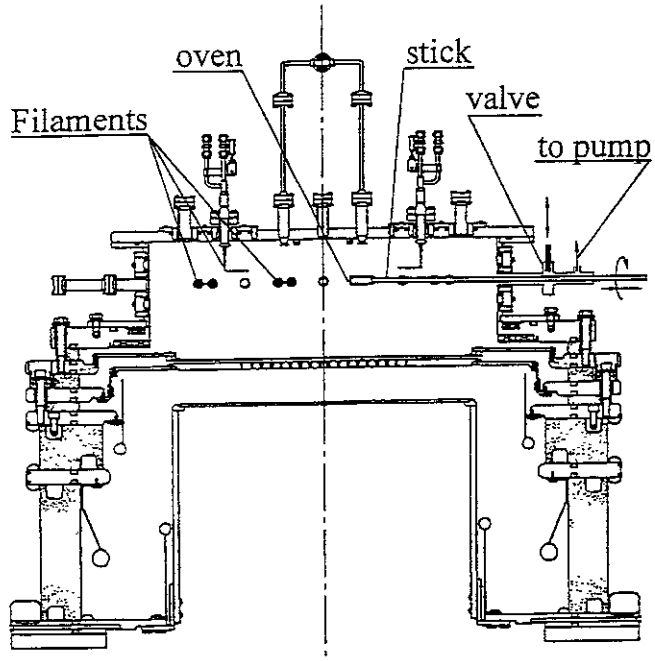

Fig.1. A schematic diagram of the 1/3 scale ion source with the cesium oven introduced

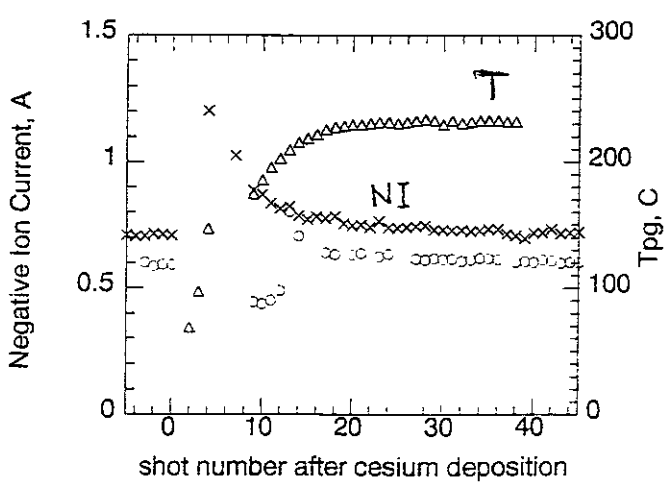

Fig.2. H- beam current evolution after 3 mg cesium depositions
circles - first 3 mg deposition,
crosses - third deposition of 3 mg portion,
T - PG temperature in third 3 mg deposition (triangles).

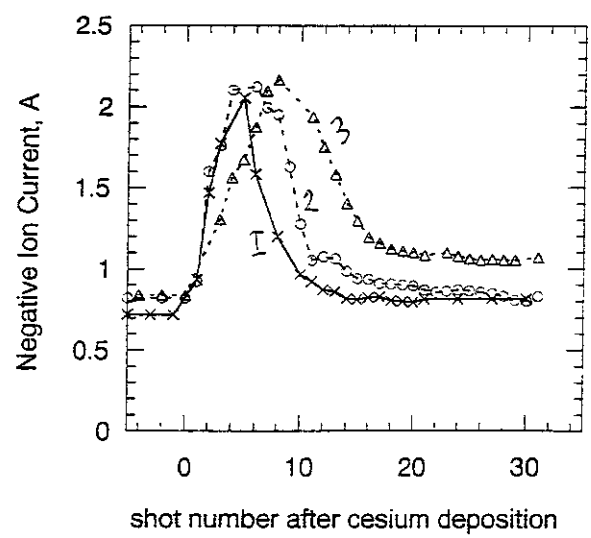

Fig.3. H- beam current evolution after 10-30 mg cesium depositior
1- 10 mg deposition (crosses),
2 - 30 mg portion (circles),
3 - third deposition of 30 mg portion (triangles).

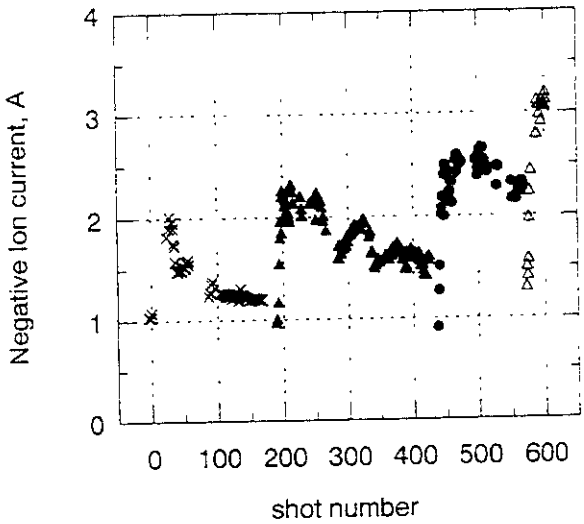

Fig.4. H- beam current evolution after 0.1-0.2 g cesium depositions.

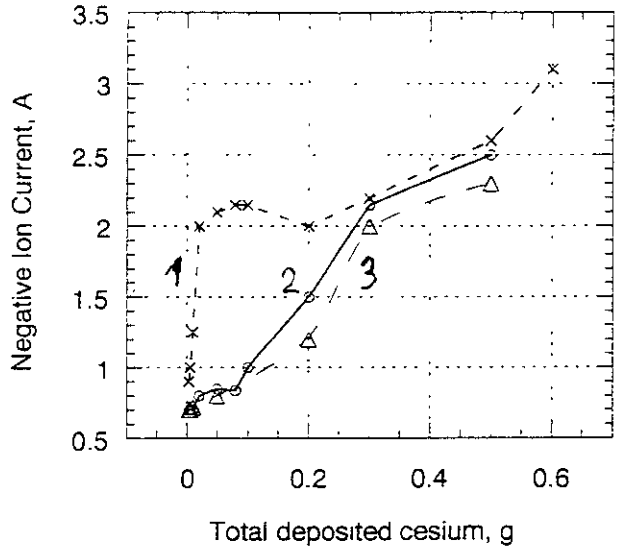

Fig.5. H- beam versus total deposited cesium amount
1 - at temporal maximum ~~(squares)~~; crosses
2 - at 50th shot after cesium depositions (circles)
3 - at 100th shot after cesium depositions (triangles)

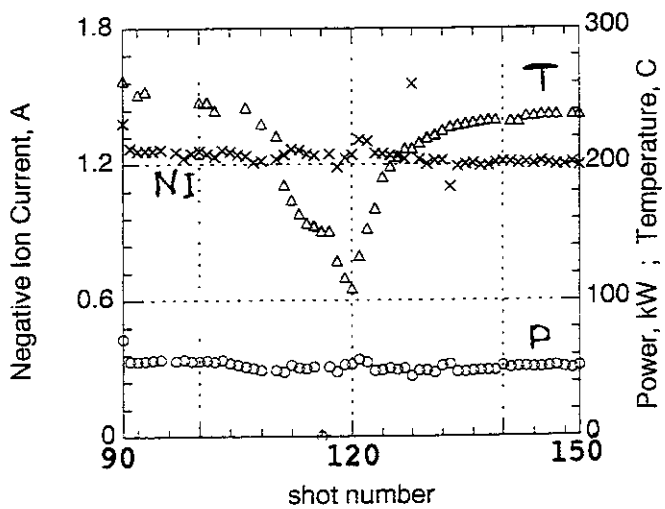

Fig.6. H- current and PG temperature evolution during operation with a longer/shorter pause between the pulses.

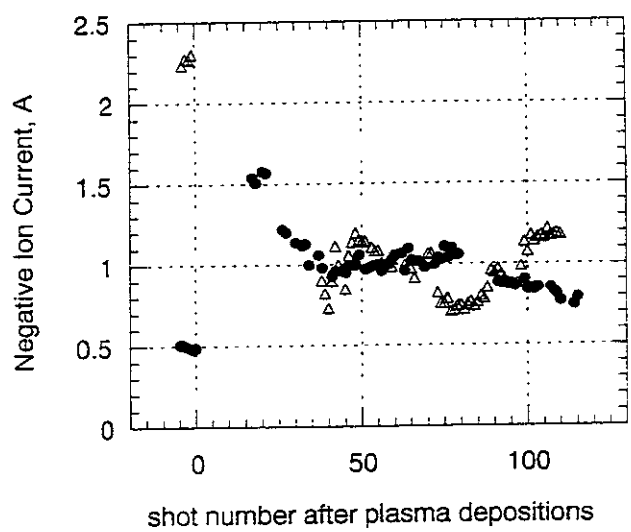

Fig.7. H- beam current evolution after cesium deposition by pla
circles - deposition to wiped wall
triangles - additional deposition over cesium

Recent Issues of NIFS Series

NIFS-557 Y Takeiri, M Osakabe, K Tsumori, Y. Oka, O Kaneko, E Asano, T Kawamoto, R. Akiyama and M Tanaka,
Development of a High-Current Hydrogen-Negative Ion Source for LHD-NBI System, Aug 1998

NIFS-558 M Tanaka, A. Yu Grosberg and T Tanaka,
Molecular Dynamics of Structure Organization of Polyampholytes, Sep 1998

NIFS-559 R Horiuchi, K. Nishimura and T Watanabe,
Kinetic Stabilization of Tilt Disruption in Field-Reversed Configurations, Sep 1998
(IAEA-CN-69/THP1/11)

NIFS-560 S. Sudo, K Kholopenkov, K. Matsuoka, S. Okamura, C. Takahashi, R. Akiyama, A Fujisawa, K Ida, H Idei, H Iguchi, M Isobe, S Kado, K. Kondo, S. Kubo, H Kuramoto, T. Minami, S Morita, S. Nishimura, M Osakabe, M. Sasao, B. Peterson, K Tanaka, K Toi and Y. Yoshimura,
Particle Transport Study with Tracer-Encapsulated Solid Pellet Injection, Oct 1998
(IAEA-CN-69/EXP1/18)

NIFS-561 A Fujisawa, H. Iguchi, S. Lee, K Tanaka, T. Minami, Y Yoshimura, M Osakabe, K Matsuoka, S. Okamura, H Idei, S Kubo S Ohdachi, S. Morita, R. Akiyama, K. Toi, H Sanuki, K Itoh, K Ida, A. Shimizu, S Takagi, C Takahashi, M. Kojima, S Hidekuma, S Nishimura, M. Isobe, A. Ejiri, N. Inoue, R. Sakamoto, Y. Hamada and M. Fujiwara,
Dynamic Behavior Associated with Electric Field Transitions in CHS Heliotron/Torsatron, Oct 1998
(IAEA-CN-69/EX5/1)

NIFS-562 S. Yoshikawa,
Next Generation Toroidal Devices; Oct. 1998

NIFS-563 Y. Todo and T. Sato,
Kinetic-Magnetohydrodynamic Simulation Study of Fast Ions and Toroidal Alfvén Eigenmodes; Oct 1998
(IAEA-CN-69/THP2/22)

NIFS-564 T Watari, T. Shimozuma, Y. Takeiri, R. Kumazawa, T. Mutoh, M. Sato, O. Kaneko, K Ohkubo, S. Kubo, H Idei, Y Oka, M. Osakabe, T. Seki, K. Tsumori, Y. Yoshimura, R. Akiyama, T Kawamoto, S. Kobayashi, F. Shimpo, Y Takita, E Asano, S Itoh G Nomura, T. Ido, M. Hamabe, M. Fujiwara, A. Iiyoshi, S Morimoto, T. Bigelow and Y P. Zhao,
Steady State Heating Technology Development for LHD; Oct. 1998
(IAEA-CN-69/FTP/21)

NIFS-565 A. Sagara, K.Y. Watanabe, K. Yamazaki, O. Motojima, M. Fujiwara, O. Mitarai, S Imagawa, H Yamanishi, H. Chikaraishi, A Kohyama, H. Matsui, T. Muroga, T. Noda, N. Ohyabu, T. Satow, A.A. Shishkin, S. Tanaka, T Terai and T Uda,
LHD-Type Compact Helical Reactors; Oct 1998
(IAEA-CN-69/FTP/03(R)

NIFS-566 N. Nakajima, J. Chen, K. Ichiguchi and M. Okamoto,
Global Mode Analysis of Ideal MHD Modes in L=2 Heliotron/Torsatron Systems, Oct 1998
(IAEA-CN-69/THP1/08)

NIFS-567 K. Ida, M. Osakabe, K. Tanaka, T. Minami, S. Nishimura, S. Okamura, A Fujisawa, Y. Yoshimura, S. Kubo, R. Akiyama, D.S Darrow, H. Idei, H. Iguchi, M. Isobe, S. Kado, T. Kondo, S Lee, K. Matsuoka, S. Morita, I. Nomura, S. Ohdachi, M Sasao A Shimizu, K. Tumori, S. Takayama, M. Takechi, S. Takagi, C. Takahashi, K Toi and T Watari,
Transition from L Mode to High Ion Temperature Mode in CHS Heliotron/Torsatron Plasmas, Oct 1998
(IAEA-CN-69/EX2/2)

NIFS-568 S. Okamura, K. Matsuoka, R Akiyama, D.S Darrow, A. Ejiri, A Fujisawa, M. Fujiwara, M. Goto, K. Ida H. Idei, H Iguchi, N. Inoue, M. Isobe, K. Itoh, S. Kado, K. Khlopenkov, T. Kondo, S Kubo, A. Lazaros, S. Lee, G. Matsunaga, T. Minami, S Morita, S Murakami, N. Nakajima, N. Nikai, S. Nishimura, I. Nomura, S. Ohdachi, K. Ohkuni, M. Osakabe, R. Pavlichenko, B. Peterson, R. Sakamoto, H. Sanuki, M. Sasao, A. Shimizu, Y. Shirai, S. Sudo, S Takagi, C Takahashi, S. Takayama, M. Takechi, K Tanaka, K Toi, K. Yamazaki, Y. Yoshimura and T. Watari,
Confinement Physics Study in a Small Low-Aspect-Ratio Helical Device CHS; Oct. 1998
(IAEA-CN-69/OV4/5)

NIFS-569 M.M. Skoric, T. Sato, A. Maluckov, M.S Jovanovic,
Micro- and Macro-scale Self-organization in a Dissipative Plasma; Oct 1998

NIFS-570 T Hayashi, N. Mizuguchi, T-H Watanabe, T. Sato and the Complexity Simulation Group,
Nonlinear Simulations of Internal Reconnection Event in Spherical Tokamak, Oct 1998
(IAEA-CN-69/TH3/3)

NIFS-571 A Iiyoshi, A. Komori, A. Ejiri, M. Emoto, H. Funaba, M. Goto, K. Ida, H. Idei, S. Inagaki, S Kado, O. Kaneko, K Kawahata, S Kubo, R. Kumazawa, S. Masuzaki, T. Minami, J. Miyazawa, T. Morisaki, S Morita, S. Murakami, S. Muto, T Muto, Y Nagayama, Y. Nakamura, H. Nakanishi, K. Narihara, K. Nishimura, N. Noda, T Kobuchi, S. Ohdachi, N Ohyabu, Y. Oka, M Osakabe,

T. Ozaki, B.J. Peterson, A. Sagara, S Sakakibara, R. Sakamoto, H. Sasao, M. Sasao, K. Sato, M. Sato, T. Seki, T Shimozuma, M. Shoji, H. Suzuki, Y Takeiri, K. Tanaka, K. Toi, T. Tokuzawa, K. Tsumori, I Yamada, H. Yamada, S. Yamaguchi, M. Yokoyama, K Y.Watanabe, T. Watari, R. Akiyama, H. Chikaraishi, K. Haba, S. Hamaguchi, S. Iima, S. Imagawa, N. Inoue, K Iwamoto, S Kitagawa, Y. Kubota, J. Kodaira, R Maekawa, T. Mito. T. Nagasaka, A. Nishimura, Y Takita, C. Takahashi, K Takahata, K Yamauchi, H. Tamura, T. Tsuzuki, S. Yamada, N. Yanagi, H. Yonezu, Y. Hamada, K. Matsuoka, K. Murai, K Ohkubo, I. Ohtake, M. Okamoto, S. Sato, T. Satow, S. Sudo, S. Tanahashi, K. Yamazaki, M. Fujiwara and O. Motojima,
An Overview of the Large Helical Device Project; Oct. 1998
(IAEA-CN-69/OV1/4)

NIFS-572 M. Fujiwara, H. Yamada, A. Ejiri, M. Emoto, H. Funaba, M. Goto, K. Ida, H. Idei, S. Inagaki, S. Kado, O. Kaneko, K. Kawahata, A. Komori, S. Kubo, R. Kumazawa, S. Masuzaki, T Minami, J. Miyazawa, T. Morisaki, S. Morita, S Murakami, S Muto, T Muto, Y. Nagayama, Y. Nakamura, H. Nakanishi, K. Narihara, K. Nishimura, N. Noda, T. Kobuchi, S. Ohdachi, N. Ohyabu, Y. Oka, M. Osakabe, T. Ozaki, B. J. Peterson, A. Sagara, S. Sakakibara, R. Sakamoto, H. Sasao, M. Sasao, K. Sato, M. Sato, T. Seki, T. Shimozuma, M. Shoji, H. Sazuki, Y. Takeiri, K. Tanaka, K. Toi, T. Tokuzawa, K. Tsumori, I. Yamada, S. Yamaguchi, M. Yokoyama, K.Y. Watanabe, T. Watari, R. Akiyama, H. Chikaraishi, K. Haba, S. Hamaguchi, M. Iima, S. Imagawa, N Inoue, K. Iwamoto, S. Kitagawa, Y. Kubota, J. Kodaira, R. Maekawa, T. Mito, T. Nagasaka, A. Nishimura, Y. Takita, C Takahashi, K. Takahata, K. Yamauchi, H. Tamura, T. Tsuzuki, S. Yamada, N Yanagi, H. Yonezu, Y. Hamada, K. Matsuoka, K. Murai, K. Ohkubo, I. Ohtake, M. Okamoto, S. Sato, T Satow, S Sudo, S. Tanahashi, K. Yamazaki, O Motojima and A. Iiyoshi,
Plasma Confinement Studies in LHD; Oct 1998
(IAEA-CN-69/EX2/3)

NIFS-573 O. Motojima, K. Akaishi, H. Chikaraishi, H. Funaba, S. Hamaguchi, S. Imagawa, S. Inagaki, N. Inoue, A. Iwamoto, S. Kitagawa, A. Komori, Y Kubota, R. Maekawa, S. Masuzaki, T. Mito, J. Miyazawa, T. Monsaki, T. Muroga, T. Nagasaka, Y Nakmura, A. Nishimura, K. Nishimura, N. Noda, N. Ohyabu, S. Sagara, S. Sakakibara, R. Sakamoto, S. Satoh, T. Satow, M. Shoji, H Suzuki, K. Takahata, H. Tamura, K. Watanabe, H. Yamada, S. Yamada, S. Yamaguchi, K. Yamazaki, N. Yanagi, T. Baba, H Hayashi, M. Iima, T. Inoue, S. Kato, T. Kato, T. Kondo, S. Monuchi, H. Ogawa, I. Ohtake, K. Ooba, H. Sekiguchi, N. Suzuki, S Takami, Y. Taniguchi, T. Tsuzuki, N. Yamamoto, K. Yasui, H. Yonezu, M. Fujiwara and A. Iiyoshi,
Progress Summary of LHD Engineering Design and Construction; Oct. 1998
(IAEA-CN-69/FT2/1)

NIFS-574 K. Toi, M. Takechi, S. Takagi, G. Matsunaga, M. Isobe, T Kondo, M. Sasao, D.S Darrow, K Ohkuni, S Ohdachi R Akiyama A. Fujisawa, M. Gotoh, H Idei, K. Ida, H. Iguchi, S. Kado, M. Kojima, S Kubo, S Lee, K. Matsuoka T. Minami, S. Morita, N Nikai, S. Nishimura, S. Okamura, M. Osakabe, A. Shimizu, Y Shirai, C. Takahashi, K Tanaka, T. Watari and Y. Yoshimura,
Global MHD Modes Excited by Energetic Ions in Heliotron/Torsatron Plasmas;Oct 1998
(IAEA-CN-69/EXP1/19)

NIFS-575 Y. Hamada, A. Nishizawa, Y. Kawasumi, A. Fujisawa, M. Kojima, K. Narihara, K. Ida, A. Ejiri, S. Ohdachi, K. Kawahata, K. Toi, K. Sato, T. Seki, H. Iguchi, K. Adachi, S. Hidekuma, S.Hirokura, K. Iwasaki, T. Ido, R. Kumazawa, H. Kuramoto, T Minami, I.. Nomura, M. Sasao, K.N. Sato, T. Tsuzuki, I Yamada and T. Watari,
Potential Turbulence in Tokamak Plasmas;Oct. 1998
(IAEA-CN-69/EXP2/14)

NIFS-576 S. Murakami, U. Gasparino, H. Idei, S. Kubo, H. Maassberg, N. Marushchenko, N. Nakajima, M. Romé and M. Okamoto,
5D Simulation Study of Suprathermal Electron Transport in Non-Axisymmetric Plasmas;Oct. 1998
(IAEA-CN-69/THP1/01)

NIFS-577 S. Fujiwara and T. Sato,
Molecular Dynamics Simulation of Structure Formation of Short Chain Molecules, Nov. 1998

NIFS-578 T. Yamagishi,
Eigenfunctions for Vlasov Equation in Multi-species Plasmas Nov. 1998

NIFS-579 M. Tanaka, A. Yu Grosberg and T. Tanaka,
Molecular Dynamics of Strongly-Coupled Multichain Coulomb Polymers in Pure and Salt Aqueous Solutions;Nov. 1998

NIFS-580 J. Chen, N. Nakajima and M. Okamoto,
Global Mode Analysis of Ideal MHD Modes in a Heliotron/Torsatron System: I. Mercier-unstable Equilibria;Dec. 1998

NIFS-581 M. Tanaka, A. Yu Grosberg and T. Tanaka,
Comparison of Multichain Coulomb Polymers in Isolated and Periodic Systems: Molecular Dynamics Study; Jan. 1999

NIFS-582 V.S. Chan and S. Murakami,
Self-Consistent Electric Field Effect on Electron Transport of ECH Plasmas; Feb. 1999

NIFS-583 M. Yokoyama, N. Nakajima, M. Okamoto, Y. Nakamura and M. Wakatani,
Roles of Bumpy Field on Collisionless Particle Confinement in Helical-Axis Heliotrons;Feb. 1999

NIFS-584 T.-H. Watanabe, T. Hayashi, T. Sato, M. Yamada and H. Ji,
Modeling of Magnetic Island Formation in Magnetic Reconnection Experiment, Feb. 1999

NIFS-585 R. Kumazawa, T. Mutoh, T. Seki, F. Shinpo, G. Nomura, T. Ido, T. Watari, Jean-Marie Noterdaeme and Yangping Zhao,
Liquid Stub Tuner for Ion Cyclotron Heating; Mar. 1999

NIFS-586 A. Sagara, M. Iima, S. Inagaki, N. Inoue, H. Suzuki, K. Tsuzuki, S. Masuzaki, J. Miyazawa, S. Morita, Y. Nakamura, N. Noda, B. Peterson, S. Sakakibara, T. Shimozuma, H. Yamada, K. Akaishi, H. Chikaraishi, H. Funaba, O. Kaneko, K. Kawahata, A. Komori, N. Ohyabu, O. Motojima, LHD Exp. Group 1, LHD Exp. Group 2,
Wall Conditioning at the Starting Phase of LHD, Mar. 1999

NIFS-587 T. Nakamura and T. Yabe,
Cubic Interpolated Propagation Scheme for Solving the Hyper-Dimensional Vlasov-Poisson Equation in Phase Space, Mar. 1999

NIFS-588 W.X. Wnag, N. Nakajima, S. Murakami and M. Okamoto,
An Accurate δf Method for Neoclassical Transport Calculation, Mar. 1999

NIFS-589 K. Kishida, K. Araki, S. Kishiba and K. Suzuki,
Local or Nonlocal? Orthonormal Divergence-free Wavelet Analysis of Nonlinear Interactions in Turbulence; Mar. 1999

NIFS-590 K. Araki, K. Suzuki, K. Kishida and S. Kishiba,
Multiresolution Approximation of the Vector Fields on T^3, Mar. 1999

NIFS-591 K. Yamazaki, H. Yamada, K.Y.Watanabe, K. Nishimura, S. Yamaguchi, H. Nakanishi, A. Komori, H. Suzuki, T. Mito, H. Chikaraishi, K. Murai, O. Motojima and the LHD Group,
Overview of the Large Helical Device (LHD) Control System and Its First Operation; Apr. 1999

NIFS-592 T. Takahashi and Y. Nakao,
Thermonuclear Reactivity of D-T Fusion Plasma with Spin-Polarized Fuel, Apr. 1999

NIFS-593 H. Sugama,
Damping of Toroidal Ion Temperature Gradient Modes; Apr. 1999

NIFS-594 Xiaodong Li,
Analysis of Crowbar Action of High Voltage DC Power Supply in the LHD ICRF System, Apr. 1999

NIFS-595 K. Nishimura, R. Horiuchi and T. Sato,
Drift-kink Instability Induced by Beam Ions in Field-reversed Configurations; Apr. 1999

NIFS-596 Y. Suzuki, T.-H. Watanabe, T. Sato and T. Hayashi,
Three-dimensional Simulation Study of Compact Toroid Plasmoid Injection into Magnetized Plasmas; Apr. 1999

NIFS-597 H. Sanuki, K. Itoh, M. Yokoyama, A. Fujisawa, K. Ida, S. Toda, S.-I. Itoh, M. Yagi and A. Fukuyama,
Possibility of Internal Transport Barrier Formation and Electric Field Bifurcation in LHD Plasma, May 1999

NIFS-598 S. Nakazawa, N. Nakajima, M. Okamoto and N. Ohyabu,
One Dimensional Simulation on Stability of Detached Plasma in a Tokamak Divertor, June 1999

NIFS-599 S. Murakami, N. Nakajima, M. Okamoto and J. Nhrenberg,
Effect of Energetic Ion Loss on ICRF Heating Efficiency and Energy Confinement Time in Heliotrons, June 1999

NIFS-600 R. Horiuchi and T. Sato,
Three-Dimensional Particle Simulation of Plasma Instabilities and Collisionless Reconnection in a Current Sheet, June 1999

NIFS-601 W. Wang, M. Okamoto, N. Nakajima and S. Murakami,
Collisional Transport in a Plasma with Steep Gradients; June 1999

NIFS-602 T. Mutoh, R. Kumazawa, T. Saki, K. Saito, F. Simpo, G. Nomura, T. Watari, X. Jikang, G. Cattanei, H. Okada, K. Ohkubo, M. Sato, S. Kubo, T. Shimozuma, H. Idei, Y. Yoshimura, O. Kaneko, Y. Takeiri, M. Osakabe, Y. Oka, K. Tsumori, A. Komori, H. Yamada, K. Watanabe, S. Sakakibara, M. Shoji, R. Sakamoto, S. Inagaki, J. Miyazawa, S. Morita, K. Tanaka, B.J. Peterson, S. Murakami, T.

Minami, S. Ohdachi, S. Kado, K. Nanhara, H. Sasao, H. Suzuki, K. Kawahata, N. Ohyabu, Y. Nakamura, H. Funaba, S Masuzaki, S. Muto, K. Sato, T. Morisaki, S. Sudo, Y. Nagayama, T. Watanabe, M. Sasao, K.. Ida, N. Noda, K. Yamazaki, K. Akaishi, A. Sagara, K. Nishimura, T. Ozaki, K. Toi, O. Motojima, M. Fujiwara, A. Iiyoshi and LHD Exp. Group 1 and 2,
First ICRF Heating Experiment in the Large Helical Device; July 1999

NIFS-603 P.C. de Vries, Y. Nagayama, K. Kawahata, S. Inagaki, H. Sasao and K. Nagasaki,
Polarization of Electron Cyclotron Emission Spectra in LHD; July 1999

NIFS-604 W. Wang, N. Nakajima, M. Okamoto and S Murakami,
δf Simulation of Ion Neoclassical Transport; July 1999

NIFS-605 T. Hayashi, N. Mizuguchi, T. Sato and the Complexity Simulation Group,
Numerical Simulation of Internal Reconnection Event in Spherical Tokamak; July 1999

NIFS-606 M Okamoto, N. Nakajima and W Wang,
On the Two Weighting Scheme for δf Collisional Transport Simulation, Aug. 1999

NIFS-607 O. Motojima, A.A. Shishkin, S. Inagaki, K. Y. Watanabe,
Possible Control Scenario of Radial Electric Field by Loss-Cone-Particle Injection into Helical Device; Aug. 1999

NIFS-608 R. Tanaka, T. Nakamura and T. Yabe,
Constructing Exactly Conservative Scheme in Non-conservative Form; Aug. 1999

NIFS-609 H Sugama,
Gyrokinetic Field Theory; Aug. 1999

NIFS-610 M. Takechi, G. Matsunaga, S. Takagi, K.Ohkuni, K Toi, M Osakabe, M. Isobe, S. Okamura, K Matsuoka, A Fujisawa, H Iguchi, S. Lee, T. Minami, K. Tanaka, Y Yoshimura and CHS Group,
Core Localized Toroidal Alfven Eigenmodes Destabilized By Energetic Ions in the CHS Heliotron/Torsatron; Sep. 1999

NIFS-611 K. Ichiguchi,
MHD Equilibrium and Stability in Heliotron Plasmas; Sep. 1999

NIFS-612 Y. Sato, M. Yokoyama, M. Wakatani and V. D. Pusovitov,
Complete Suppression of Pfirsch-Schluter Current in a Toroidal l=3 Stellarator; Oct. 1999

NIFS-613 S. Wang, H. Sanuki and H. Sugama,
Reduced Drift Kinetic Equation for Neoclassical Transport of Helical Plasmas in Ultra-low Collisionality Regime; Oct. 1999

NIFS-614 J. Miyazawa, H. Yamada, K. Yasui, S. Kato, N., Fukumoto, M. Nagata and T Uyama,
Design of Spheromak Injector Using Conical Accelerator for Large Helical Device; Nov. 1999

NIFS-615 M. Uchida, A. Fukuyama, K. Itoh, S.-I. Itoh and M. Yagi,
Analysis of Current Diffusive Ballooning Mode in Tokamaks; Dec. 1999

NIFS-616 M. Tanaka, A.Yu Grosberg and T. Tanaka,
Condensation and Swelling Behavior of Randomly Charged Multichain Polymers by Molecular Dynamics Simulations; Dec. 1999

NIFS-617 S. Goto and S. Kida,
Sparseness of Nonlinear Coupling; Dec. 1999

NIFS-618 M.M. Skoric, T. Sato, A. Maluckov and M.S. Jovanovic,
Complexity in Laser Plasma Instabilities Dec. 1999

NIFS-619 T.-H. Watanabe, H. Sugama and T. Sato,
Non-dissipative Kinetic Simulation and Analytical Solution of Three-mode Equations of Ion Temperature Gradient Instability; Dec. 1999

NIFS-620 Y. Oka, Y. Takeiri, Yu.I.Belchenko, M. Hamabe, O. Kaneko, K. Tsumori, M. Osakabe, E. Asano, T. Kawamoto, R. Akiyama,
Optimization of Cs Deposition in the 1/3 Scale Hydrogen Negative Ion Source for LHD-NBI System ;Dec. 1999